

EUROPEAN COOPERATION
IN THE FIELD OF SCIENTIFIC
AND TECHNICAL RESEARCH

COST 2100 TD(09) 928
Vienna, Austria
September 28–30, 2009

EURO-COST

SOURCE:

¹Institut für Nachrichten- und Hochfrequenztechnik, Technische Universität Wien, Vienna, Austria

²Forschungszentrum Telekommunikation Wien (ftw.), Vienna, Austria

³Department of Electrical and Information Technology, Lund University, Lund, Sweden

⁴Delphi Delco Electronics Europe GmbH, Bad Salzdetfurth, Germany

⁵Volkswagen AG, Wolfsburg, Germany

Overview of Vehicle-to-Vehicle Radio Channel Measurements for Collision Avoidance Applications

Alexander Paier¹, Laura Bernadó², Johan Karedal³, Oliver Klemp⁴,
Andreas Kwoczek⁵, Fredrik Tufvesson³, Andreas Thiel⁴, Yi Zhou²,
Nicolai Czink², Thomas Zemen², Andreas F. Molisch³,
Christoph F. Mecklenbräuer¹

¹Institut für Nachrichten- und Hochfrequenztechnik
Gusshausstrasse 25/389
1040 Vienna
AUSTRIA

Phone: +43 1 58801 38951

Fax: +43 1 58801 38999

Email: apaier@nt.tuwien.ac.at

Overview of Vehicle-to-Vehicle Radio Channel Measurements for Collision Avoidance Applications

Alexander Paier¹, Laura Bernadó², Johan Karedal³, Oliver Klemp⁴, Andreas Kwoczek⁵, Fredrik Tufvesson³, Andreas Thiel⁴, Yi Zhou², Nicolai Czink², Thomas Zemen², Andreas F. Molisch³, Christoph F. Mecklenbräuer¹

¹Institut für Nachrichtentechnik und Hochfrequenztechnik, Technische Universität Wien, Vienna, Austria

²Forschungszentrum Telekommunikation Wien (ftw.), Vienna, Austria

³Department of Electrical and Information Technology, Lund University, Lund, Sweden

⁴Delphi Delco Electronics Europe GmbH, Bad Salzdetfurth, Germany

⁵Volkswagen AG, Wolfsburg, Germany

Contact: apaier@nt.tuwien.ac.at

Abstract—In this contribution we present an overview of a vehicle-to-vehicle radio channel measurement campaign at 5.6 GHz. Evaluations of an overtaking in traffic congestion situation for collision avoidance, and general line of sight obstruction between a transmitter and a receiver car show that in this situation the radio channel is highly influenced by the rich scattering environment.

I. INTRODUCTION

Vehicle-to-vehicle (V2V) communications systems have recently drawn great attention, because they have the potential to reduce traffic jams and accident rates. The simulation and performance evaluation of existing systems like IEEE 802.11p, as well as the design of future, improved systems, requires a deep understanding of the underlying propagation channels. V2V communications also gained more importance by the European committee decision on the harmonized use of the 5875 – 5905 MHz frequency band for safety-related applications of intelligent transport systems (ITS), [1]. Realistic V2V radio channel measurements are rare, e.g. [2], [3], [4]. Based on the experience from a first V2V radio channel measurement campaign [5] in 2007, we carried out an improved V2V channel measurement campaign, called *DRIVEWAY* in June 2009, with following special features: multiple-input multiple-output (MIMO) and single-input single-output (SISO) measurements, realistic vehicular antennas calibrated including its mounting on the car, sophisticated rubidium clock synchronised channel sounder, and up to 78 kHz maximum resolvable Doppler shift. A novelty of this measurement campaign is that we chose the scenarios and situations for the most important safety-related ITS applications, based on the information in [ref: PRE-DRIVE, COMeSafety]. This paper presents an overview of the measurements and first results from selected collision avoidance application scenarios.

II. MEASUREMENTS

A. Measurement Equipment

For our channel measurements, we used the sophisticated RUSK LUND channel sounder that performs MIMO mea-

surements based on the “switched-array” principle. We were measuring with a large bandwidth of 240 MHz at a center frequency of 5.6 GHz. This center frequency was the highest possible to select on the channel sounder and is very close to the allocated 5.9 GHz frequency band for ITS in Europe. We do not expect a different behaviour of the radio channel between 5.6 GHz and 5.9 GHz. The transmit power was set to 27 dBm. Depending on the driving situation (e.g. speed of the cars) we were varying several parameters of the channel sounder, in order to achieve the most suitable resolutions and results. Beside the MIMO measurements with 4 transmit and 4 receive antenna elements, resulting in a total number of 16 measured links, we also carried out SISO measurements, in order to sample the radio channel as fast as possible. Based on this parameter settings we achieved a maximum resolvable Doppler shift between 1.6 kHz and 78 kHz. The channel sounder provides the sampled transfer function $H[m, q]$ with discrete time index m and discrete frequency index q .

For the measurement campaign, an application-specific antenna module was designed and integrated into the vehicular environment. The antenna module consists of $N = 4$ identical elements in a uniform linear array (ULA) configuration featuring interelement spacings of $\lambda/2$. The array elements are given by circular patch antennas that are excited in a higher-operational mode yielding terrestrial beam patterns with vertical polarization. Identical antenna modules are used for the transmitter (Tx) and -receiver (Rx) cars. Following the conventional mounting position for roof-top antennas on the rear part of the vehicle, custom *Volkswagen Touran* measurement vehicles were equipped with the antenna modules. The ULA orientation was chosen perpendicular to driving direction. Calibrated in-situ antenna measurements were taken in a large automated antenna measurement facility. Figure 1 shows the Rx of the channel sounder packed in the trunk of the car.



Fig. 1. Rx car.

B. Measurement Scenarios

The measurements were carried out in the cities of Lund and Malmö, both in Sweden. The scenario and situation selection was application based. We chose the scenarios and situations that are most important for safety-related ITS applications:

- **Road crossing:** The measurement cars are approaching a road crossing from perpendicular roads in four different environments. The first environment is an open area road crossing. In the other three environments there is obstructed line of sight (LOS) at the beginning of the measurements. Besides the obstructed LOS there is either an open surrounding area or surrounding buildings, where in the latter case a single lane and multiple lane scenario are considered.
- **General LOS obstructions:** Both measurement cars are driving in the same direction on the highway, where trucks are blocking the LOS.
- **Merging lanes:** The Rx car is driving on the highway and the Tx car is entering the highway on a partly obstructed entrance ramp.
- **Traffic congestion:** Different situations in a traffic congestion are considered, e.g. both cars are stuck in the traffic congestion, one car is overtaking the other one, and one car is approaching the traffic congestion, where the other car is stuck.
- **In-tunnel:** The measurements are carried out on the famous Öresund bridge-tunnel, where both cars are driving in the same direction with different distances and varying number of cars between them.
- **Investigation of ground reflection:** With these measurements we investigate the behavior of the radio channel on dry and wet roads in static scenarios, i.e. when both cars are parked. Further we compare a driving-by scenario from this measurement campaign with measurements in the same scenario from the first measurement campaign, [5], where we used different antenna heights, antennas, and vehicles.
- **Influence of array orientation:** These measurements are not related to specific applications, but are carried out in

order to investigate the influence of linear antenna array orientation, e.g. on channel capacity or spatial diversity. For this purpose, a static scenario where both cars are parked either parallel or perpendicular to the road, and a mobile scenario where the Rx car is passing the parked (parallel or perpendicular) Tx car are considered. These situations were measured in a rural as well as in an urban environment.

Except of the last two scenarios all scenarios are strongly related to safety-related ITS applications, e.g.

- collision avoidance,
- emergency vehicle warning,
- pre-crash sensing warning,
- hazardous location notification,
- wrong way driving warning,
- co-operative merging assistance,
- traffic condition warning,
- stationary vehicle warning,
- slow vehicle warning,
- lane change assistance,
- co-operative forward collision warning, and
- overtaking vehicle warning.

III. MEASUREMENT RESULTS

The focus of this section is the general behaviour of the vehicular radio channel in different scenarios. We do not provide directional or MIMO results in this paper.

In vehicular communications the observed fading processes are non-stationary. We can assume that the process is stationary for a given period in time, which is labeled with the variable k , then it is meaningful to represent its power spectral density as a function of time. In this sense, we compute an estimate of the local scattering function $\hat{C}_H[k; p, n]$ as in [6], which will allow us to calculate the time-variant power-delay profile (PDP) and Doppler spectral density (DSD). The ranges of the delay n and Doppler shift p are $\{0, \dots, N - 1\}$ and $\{-M/2, \dots, M/2 - 1\}$ respectively. The number of temporal samples m of the measured channel transfer function $H[m, q]$ is S , and the number of frequency samples q is Q . The absolute time m and the time index of the stationary region k are related by $m = Mk + m'$, where $k = 0 \dots \lfloor S/M \rfloor - 1$ and $m' = 0 \dots M - 1$.

The time-variant PDP

$$PDP[k; n] = \sum_{l=1}^L \sum_{\nu=-M/2}^{M/2-1} \hat{C}_H^{(l)}[k; p, n], \quad (1)$$

and time-variant DSD

$$DSD[k; p] = \sum_{l=1}^L \sum_{\tau=0}^{N-1} \hat{C}_H^{(l)}[k; p, n], \quad (2)$$

are obtained by summing the PDPs and the DSDs of all measured MIMO links $l = 1 \dots L$.

In this paper we evaluate the PDP and DSD of two different scenarios. The first one is an overtaking in a traffic congestion situation, and the second scenario is a general obstructed LOS produced by a truck between Tx and Rx car.

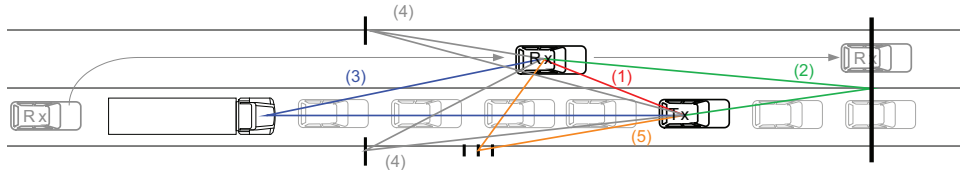


Fig. 4. Scatterers distribution for scenario 1.

A. Scenario 1:

Figure 2 and 3 show the PDP and DSD for an overtaking scenario in a traffic congestion situation. During the measurement run the Tx is stuck in a traffic jam on the right lane, whereas the Rx overtakes the Tx on the left lane. This situation is of special interest from the traffic safety point of view. It is a common reaction that a car stuck in a traffic jam on only one lane decides suddenly to change lane, sometimes without enough visibility. We analyze different scattering

truck and moves to the left in order to overtake the Tx. We observe in Fig. 2 how the delay corresponding to this path gets smaller until the Rx overtakes the Tx at 14.3 s. At this time the delay is the shortest, corresponding to a distance between cars of about 4 m. In Fig. 3 the Doppler shift is 0 Hz in the beginning, when both cars are on the right lane and stuck in the traffic jam. It increases towards positive values when the Rx starts overtaking. Between 3.5 and 14.3 s, the two cars are approaching and therefore the Doppler shift is positive. From 14.3 s on, the Rx has passed the Tx and drives away from it, thus observing a negative Doppler shift. At the end of the measurement, the Rx breaks due to a congestion also on the left lane and, as a result, the Doppler shift decreases to 0 Hz. The maximum Doppler shift observed for the LOS path is 292 Hz which corresponds to a speed of 56 km/h, which was the speed of the Rx during the overtaking.

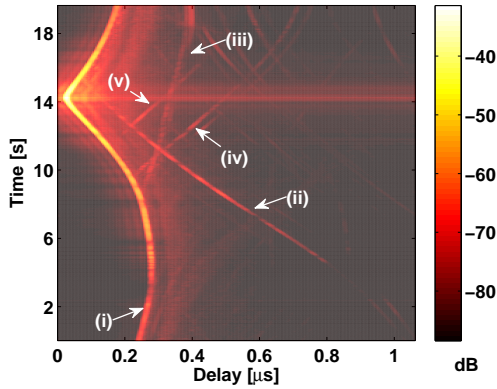


Fig. 2. PDP: Overtaking in traffic congestion.

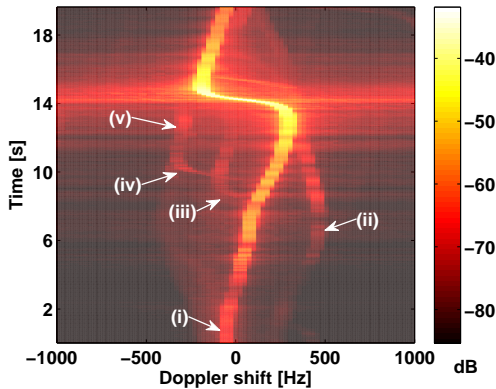


Fig. 3. DSD: Overtaking in traffic congestion.

contributions in the PDP and DSD, labeled in Fig. 2 and 3 from (i) to (v). Figure 4 shows a scheme of how the mobile and static scatterers are distributed. Contribution (i) corresponds to the LOS between the Tx and Rx car. In the beginning, the Rx stays on the right lane behind a large

Path (ii) corresponds to a single bounce reflection produced by a big traffic sign placed ahead of both cars. This contribution occurs at 4.3 s. The Rx is not able to receive it earlier because there is a big truck blocking the signal coming from this direction. The maximum Doppler shift is 445 Hz, that means a relative speed of 85 km/h. At this point, Tx and Rx are driving about 25 km/h and 60 km/h respectively.

The large truck standing in front of the Rx in the beginning of the measurement causes multipath contribution (iii). When the Rx overtakes this truck, at 8.7 s, it is possible to detect a further contribution. Then, Tx and Rx leave the truck behind and therefore the observed delay increases and the Doppler shift is negative. The maximum Doppler shift observed on this path corresponds to a relative speed of 17 km/h.

A similar phenomenon happens for paths (iv) and (v). They correspond to temporary traffic signs at both sides of the road which contribute to the received signal as soon as they are left behind. Since both Tx and Rx are leaving these objects, the observed Doppler shift is negative and the delay increases.

The other cars present in the measurement contribute to the received signal with a slightly longer delay path than the LOS path, therefore we are not able to separate them from the LOS.

B. Scenario 2:

Next, we present the evaluations for the second scenario described in Fig. 6. The Rx drives in front of a truck at about 80 km/h and the Tx is behind this truck and drives at about 65 km/h. This is a typical situation of obstructed LOS, where the first path between Tx and Rx happens through diffraction on the roof surface of the truck. Figures 7 and 8 show the PDP and DSD observed for this scenario where we identify 5 different scattering contributions. As done for scenario 1, we

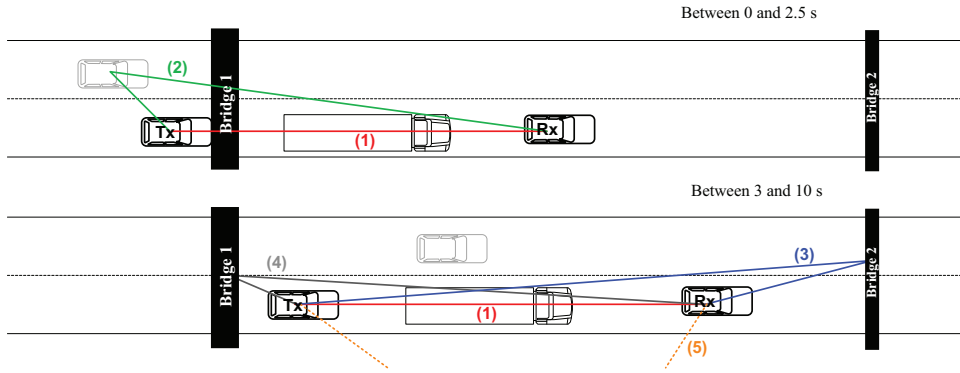


Fig. 6. Scatterers distribution for scenario 2.

label these multipath contributions in the figures.

The first path corresponds to the obstructed LOS between Tx and Rx. It has a slightly shorter delay than the one the direct path would have. Since the Rx drives faster than the Tx, the delay of this path grows with time. Noteworthy are three intervals in which the signal strength increases. The first interval starts at time 0 s and lasts until 3 s and corresponds to the time while there is a bridge between Tx and Rx. The same phenomena happens during the second interval, between 4.5 and 5.5 s when the Rx, which drives in the front, goes through a second smaller bridge. We observe again the effect of the bridge at 9.5 s, there the Tx drives under the second bridge. The transmission benefits from having these strongly reflecting bridges on the way. The reflections produced by these objects contribute to increasing the received power at the Rx.

For the first path, the observed Doppler shift is slightly shifted towards negative values. The Rx drives between 10 and 15 km/h faster than the Tx, the observed Doppler shift is -63.5 Hz, well matching with a relative speed of 12 km/h. During the measurement run, the Tx decreases the speed about 5 km/h at 4 s, and therefore the Doppler shift of this first path gets more negative down to -89 Hz.

Path (ii) corresponds to a car that passes the Tx at 1.1 s. Normally we cannot notice any contribution from other cars driving beside Tx and Rx. In this case, since the overtaking takes places under the bridge, this path becomes stronger at



Fig. 5. Aerial of measurement scenario 2. ©2009 Google-Map data

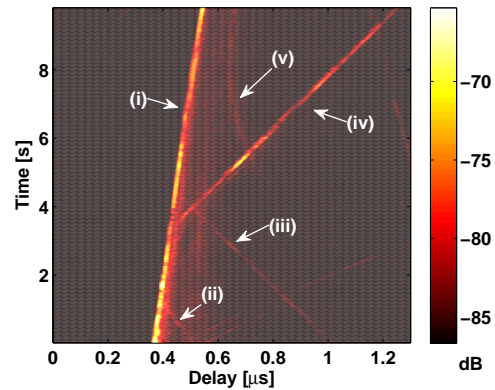


Fig. 7. PDP: Obstructed LOS.

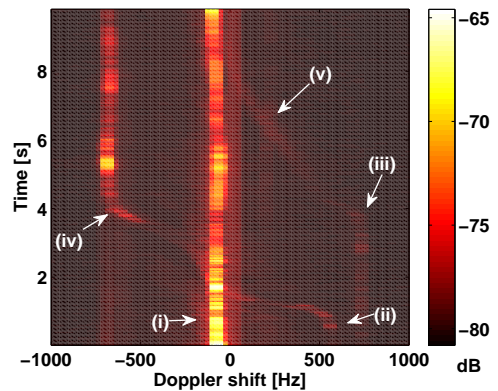


Fig. 8. DSD: Obstructed LOS.

that time. The Doppler shift associated to this path is 545 Hz, this leads to a relative speed of 105 km/h. Taking the Tx and Rx speed into account, this third car should be driving at about 124 km/h.

The third path shows a decreasing delay with time, which means that both Tx and Rx are approaching an object. At 4.5 s this object falls in between Tx and Rx geometrically, just when the Rx starts driving under the second bridge. There

is a reflection happening on the bridge when both cars are approaching it. The measured Doppler shift is 735 Hz and the relative speed to this object from both cars is about 140 km/h.

The fourth path appears shortly after the Tx leaves the first bridge, and it is produced by a reflection on this bridge. The delay increases with time and the Doppler shift is -700 Hz. The observed Doppler shift of path (*iv*) is smaller in magnitude than the one for path (*iii*) because at 4 s the Tx reduces its speed to 60 km/h. We detect a signal strength difference between paths (*iii*) and (*iv*) although both come from reflection on bridges. The first bridge is larger than the second one, the reflecting surface is therefore bigger, and consequently the reflections produced by it are stronger.

In Fig. 5 we observe a large building about 100 meters of the road. This building causes the fifth contribution. Since it is an object placed far away from the Tx and Rx, the changes on the delay and Doppler shift are smoother. The shortest delay of this path is $0.65 \mu\text{s}$ with a travelled distance of 180 m.

IV. CONCLUSION

This paper gives an overview about a recently conducted vehicle-to-vehicle radio channel measurement campaign using the RUSK LUND channel sounder. Seven different main situations, based on the importance for safety-related intelligent transport system (ITS) applications, were chosen. The paper presents the power-delay profile and the Doppler spectral density (DSD) for two different scenarios. The first one is an overtaking scenario in traffic congestion situation, whereas the second scenario is an obstructed line of sight caused by a truck between the Tx and Rx cars. In such scenarios the multipath contributions are produced by big metallic surfaces, mobile (trucks, other cars) or static (traffic signs, bridges, buildings). Contributions from scatterers are stronger when the cars drive under bridges. In both investigated scenarios, it is possible to detect the signal between Tx and Rx also when there is no direct LOS. This is specially beneficial for collision avoidance situations.

REFERENCES

- [1] "ECC decision of 14 March 2008 on the harmonised use of the 5875-5925 MHz frequency band for intelligent transport systems (ITS)," ECC Dec. (08)01, March 2008.
- [2] O. Renaudin, V.-M. Kolmonen, P. Vainikainen, and C. Oestges, "Wideband MIMO car-to-car radio channel measurements at 5.3 GHz," in *IEEE 68th Vehicular Technology Conference*, Calgary, Alberta, Canada, September 2008.
- [3] J. Kunisch and J. Pamp, "Wideband car-to-car radio channel measurements and model at 5.9 GHz," in *IEEE 68th Vehicular Technology Conference*, Calgary, Alberta, Canada, September 2008.
- [4] P. Paschalidis, M. Wisotzki, A. Kortke, W. Keusgen, and M. Peter, "A wideband channel sounder for car-to-car radio channel measurements at 5.7 GHz and results for an urban scenario," in *IEEE 68th Vehicular Technology Conference*, Calgary, Alberta, Canada, September 2008.
- [5] A. Paier, J. Karedal, N. Czink, H. Hofstetter, C. Dumard, T. Zemen, F. Tufvesson, C. F. Mecklenbräuker, and A. F. Molisch, "First results from car-to-car and car-to-infrastructure radio channel measurements at 5.2 GHz," in *International Symposium on Personal, Indoor and Mobile Radio Communications (PIMRC) 2007*, September 2007.
- [6] L. Bernadó, T. Zemen, A. Paier, J. Karedal, and B. H. Fleury, "Parametrization of the local scattering function estimator for vehicular-to-vehicular channels," in *IEEE 70th Vehicular Technology Conference. To be presented*, Anchorage, Alaska, USA, September 2009.